Contrast Enhancement of Color Images using a Multi-Objective Optimization Framework

Luis G. Moré[1], Diego P. Pinto-Roa[1], and José Luis Vázquez Noguera[1,2]

[1]*Facultad Politécnica - Universidad Nacional de Asunción*
[2]*Universidad Americana del Paraguay*
{*lmore,dpinto,jlvazquez*}*@pol.una.py*

Abstract. Contrast Enhancement(CE) is a fundamental preprocessing step for several applications, and also for further decision making processes related. This task has been addressed successfully for gray-scale images using pure Multi-Objective Optimization(MOO); nevertheless, difficulties arise when performing MOO for color images. This paper presents a pure MOO approach with automatic CE for color images, taking into account evaluation metrics better suited for color spaces, which are designed to achieve the improvement in contrast and also control the noise introduced because of the contrast variation seen during the process. A series of experiments were conducted in order to assess the correctness of this approach, and the results consist of a set of contrast enhanced images, with different compromise rates between contrast modification and noise introduction. It appears that the results obtained are promising, and the numeric values of the optimization metrics are analyzed using correlation tables and discussed using the Pareto Front obtained from these values.

Keywords: Multi-Objective optimization, Contrast Enhancement, MOPSO, CLAHE, Color Spaces.

1 Introduction

Contrast Enhancement (CE) is a fundamental preprocessing step for several image processing applications such as Medical Imaging (Computer Aided

Diagnosis [1], Computerized Tomography Imaging [2], Magnetic Resonance Imaging [3] and others), Remote Sensing [4], and so on.

Tecniques based on Histogram Equalization have been extensively proven to be valid when addressing CE problems [5, 6, 7, 8]. Meta-Heuristics such as Mono-Objective Optimization, and also Multi-Objective Optimization (MOO) have been tested successfully in order to solve CE problems on gray-scaled images [9, 10, 11, 12]. However, MOO applied to color images poses additional difficulties because it is neccesary to preserve color information present therein.

Our proposal consist in testing images transformed from RGB color space to $YCbCr$ in order to perform MMO-based CE. Contrast Limited Adaptive Histogram Equialization (CLAHE) is applied over the Y channel of the test image in order to modify contrast, and the resultant image is transformed back to RGB in order to evaluate the similarity between color channels.

The rest of the paper is organized as follows: in Section 2, the fundametal concepts for this work are presented, in Section 4 the CE problem is posed, and our approach is presented, in Section 5 the results achieved are discussed in detail, and finally in 6 some final points are remarked.

2   Theorethical Framework

This sections presents a brief introduction of the concepts used in the paper.

2.1   Color Spaces Adopted

Original images are represented using the RGB color space [13], which is a $N \times M \times 3$ array of color pixels. Every color pixel is represented by an element $[z_r \quad z_g \quad z_b]$ of the array previously mentioned, where z_r, z_g, z_b are the red, green, and blue components of the color pixel in a specific location. Original images are then transformed to the $YCbCr$ color space [13], which is a representation widely used in digital video. The main advantage is that the Y component here represents the luminance information of the image, meanwhile the Cb component represents a difference between the blue component and a reference value, and the Cr component is the difference between the red component and a reference value. Another important advantage of this representation is that the conversion from RGB, and back to RGB is straightforward:

$$\begin{bmatrix} Y \\ C_b \\ C_r \end{bmatrix} = \begin{bmatrix} 16 \\ 128 \\ 128 \end{bmatrix} + \begin{bmatrix} 65.481 & 128.553 & 24.966 \\ -37.797 & -74.203 & 112.000 \\ 112.000 & -93.786 & -18.214 \end{bmatrix} \begin{bmatrix} R \\ G \\ B \end{bmatrix} \quad (1)$$

$$\begin{bmatrix} R \\ G \\ B \end{bmatrix} = \begin{bmatrix} Y + 1.402 \cdot (C_r - 128) \\ Y - 0.34414 \cdot (C_b - 128) - 0.71414 \cdot (C_r - 128) \\ Y + 1.772 \cdot (C_b - 128) \end{bmatrix} \quad (2)$$

2.2   Contrast Limited Adaptive Histogram Equalization (CLAHE)

Contrast Limited Adaptive Histogram Equalization (CLAHE) [7] is a well known CE algorithm, designed for broad applicability in the context of digital image proccesing. CLAHE is a variation of the *Adaptive Histogram Equalization (AHE)*[6] CE algorithm. In AHE, an image is processed transforming each pixel using a function based on the histogram of its surrounding pixels, defined by a *Contextual Region* $(\mathscr{R}_x, \mathscr{R}_y)$. CLAHE limits the CE by clipping the resultant histogram based in a coefficient called *Clip Limit* $\mathscr{C}$

2.3   Multi-Objective Particle Swarm Optimization (MOPSO)

Multi-Objective Particle Swarm Optimization ($MOPSO$) [14] is a widely known metaheuristic algorithm. It is a bio-inspired metaheuristic which mimics the social behavior of bird flocking. In PSO, every potential solution of the problem being approached is called a *particle* and the actual population of solutions is called a *swarm*. Every particle $\vec{x}$ performs a search within a search space Ω, and for every generation t, every solution $\vec{x}$ is updated according to:

$$\vec{x}_i(t) = \vec{x}_i(t-1) + \vec{v}_i(t) \quad (3)$$

Here, $\vec{v}$ is a factor known as the velocity, and is given by:

$$\vec{v}_i(t) = w \cdot (t-1) + C_1 \cdot r_1 \cdot (\vec{x}_{p_i} - \vec{x}_i) + C_2 \cdot r_2 \cdot (\vec{x}_{g_i} - \vec{x}_i), \quad (4)$$

where $\vec{x}_{p_i}$ is the best solution that $\vec{x}_i$ has found so far, $\vec{x}_{g_i}$ is the best solution that the entire swarm has found at the current iteration, w is a coeficient known as the *inertia weight*, which controls the search speed rate of PSO; r_1 and r_2 are random numbers between $[0, 1]$. Finally, C_1 and C_2 are coefficient which control the weight between global and local particles during the search.

In $MOPSO$, a *constriction coefficient* χ is adopted in order to control the particle's velocity, as described below:

$$\chi = \frac{2}{2 - \varphi - \sqrt{\varphi^2 - 4\varphi}} \tag{5}$$

where

$$\varphi = \begin{cases} C_1 + C_2 & \text{if } C_1 + C_2 > 4 \\ 0, & \text{if } C_1 + C_2 \leq 4 \end{cases} \tag{6}$$

Furthermore, the velocity in $MOPSO$ is bounded by the following *velocity constriction* equation:

$$v_{i,j}(t) = \begin{cases} delta_j & \text{if } v_{i,j}(t) > delta_j \\ -delta_j, & \text{if } v_{i,j}(t) \leq delta_j \\ v_{i,j}(t), & \text{otherwise} \end{cases} \tag{7}$$

where

$$delta_j = \frac{upper\_limit_j - lower\_limit_j}{2} \tag{8}$$

2.4 Entropy of image

Entropy of image [15] is a metric that measures how much information is represented within an image. Entropy and contrast are closely related to the intensity distribution of images, so this metric is able to assess contrast variations as a consecuence of image transformations.

First, we need to define the *Histogram* of intensities of an image H as follows: Let $c_1, c_2, ..., c_n$ the count of pixels with intensity $i_1, i_2, ..., i_n$ respectively, and also let

$$p_i = \frac{c_i}{N}, \qquad \sum_{i=1}^{n} c_i = N, \qquad i = 1, 2, ..., n, \tag{9}$$

where N is the total sum of pixels shown in an image I and n is every intensity level representable by the color space of I. Then H is defined as a probability distribution in which every p_i represents the probability of occurrence of an intensity i. Then, Entropy of Image is defined as below:

$$\mathscr{H} = -\sum_{i=0}^{n-1} p_i \log_2(p_i) \qquad \mathscr{H} \in \{0, ..., \log_2(n)\} \tag{10}$$

2.5 Structural Similarity Index

The *Structural Similarity Index* (*SSIM*) [16] is a well known metric that measures important image's attributes such as *Luminance, Contrast* and *Structure*. SSIM main aim is to measure the distortion added to the image as a consecuence of the CE proccess. *SSIM* is calculated by windows, so given two images I_x and T_y which represent an original and an enhanced image, respectively, the *SSIM* index is defined as below:

$$SSIM(I,T) = \frac{(2\mu_{I_x}\mu_{T_y} + E_1)(2\sigma_{I_xT_y} + E_2)}{(\mu_{I_x}^2 + \mu_{T_y}^2 + E_1)(\sigma_{I_x}^2 + \sigma_{T_y}^2 + E_2)} \qquad SSIM \in [0,1] \quad (11)$$

where μ_{I_x}, μ_{T_y} is the intensity averages of I_x and T_y, respectively; $\sigma_{I_x}^2$ and $\sigma_{T_y}^2$ are the intensity variances for I_x and T_y, respectively; $\sigma_{I_xT_y}$ is the covariance between I_x and T_y intensities. $E_1 = (K_1L^2)$, where L is the dynamic range of intensities of image's pixels, and $K_1 \ll 1$ is a small constant; $E_2 = (K_2L)^2$, and $K_2 \ll 1$; both E_1 and E_2 are constants used to stabilize division when denominator is close to zero.

3 Formulation of the Problem Posed

Given an color input image I, with $M \times N$ pixels, and a vector $\vec{x} = (\mathscr{R}_x, \mathscr{R}_y, \mathscr{C})$, where $\mathscr{R}_x$ and $\mathscr{R}_y$ are contextual regions and $\mathscr{C}$ is the *Clip Limit*, a set of non-dominated solutions $\mathscr{X}$, which simultaneously maximize the objective functions f_1, f_2, f_3, f_4:

$$\mathscr{F} = [f_1(I, \vec{x}), f_2(I, \vec{x}), f_3(I, \vec{x}), f_4(I, \vec{x})]; \qquad f_1, f_2, f_3, f_4 \in [0,1] \quad (12)$$

where:

- T_y is the enhanced intensity map, when applying $\vec{x}$ to I_y; this is: $T_y = CLAHE(\vec{x}, I_y)$. T_y and I_y are the Y channel in the $YCbCr$ representation of I and T, respectively,

- $f_1(I, \vec{x}) = \frac{\mathscr{H}(T)}{\log_2 L}$ is the normalized Entropy of the enhanced intensity map T_y, as described above.

- $f_2(I, \vec{x}) = SSIM(I_R, T_R)$ is the *SSIM* measure between I_R and T_R. I_R and T_R are the R channel of the RGB representation of I and T, respectively.

- $f_3(I, \vec{x}) = SSIM(I_G, T_G)$ is the $SSIM$ measure between I_G and T_G. I_G and T_G are the G channel of the RGB representation of I and T, respectively.

- $f_4(I, \vec{x}) = SSIM(I_B, T_B)$ is the $SSIM$ measure between I_B and T_B. I_B and T_B are the B channel of the RGB representation of I and T, respectively.

Bounded to:

- $\mathscr{R}_x \in [2, ..., M]$ for the $\mathbb{N}$ numbers,

- $\mathscr{R}_y \in [2, ..., N]$ for the $\mathbb{N}$ numbers,

- $\mathscr{C} \in (0, ..., 1]$ for the $\mathbb{R}$ numbers.

4 Proposal

Algorithm 1 MOPSO-CLAHE

Require: Input image I, amount of particles Ω, iterations t_{max}
1: Initialize ω, c_1, c_2, $t = 0$, $lower\_limit_1$, $lower\_limit_2$, $lower\_limit_3$, $upper\_limit_1$, $upper\_limit_2$, $upper\_limit_3$, $\mathscr{X}$
2: **while** $t < t_{max}$ **do**
3:     **for** every i-th particle **do**
4:         Calculate new velocity $\vec{v_i}^t$ of the particle using equations (4) and (7)
5:         Calculate new particle position $\vec{x_i}^t$ using expression (3)
6:         $T = \text{CLAHE}(\vec{x_i}^t, I)$
7:         $f_i^t = f(I, \vec{x_i}^t)$
8:         **if** $\vec{x_i} \succ \vec{x_{p_i}}$ **then**
9:             replace $\vec{x}_{p_i}$ by $\vec{x_i}^t$
10:        **end if**
11:        **if** $\vec{x_i} \succ \vec{x_{g_i}}$ **then**
12:           Update the Pareto set $\mathscr{X}$
13:        **end if**
14:        $t = t + 1$
15:     **end for**
16: **end while**
Ensure: $\mathscr{X}$

Algorithm 1 shows how Color Multi-Objective PSO-CLAHE ($CMOPSO-CLAHE$) is implemented, in order to tune parameters of $CLAHE$. The parameters received by $CLAHE$ are stored by a particle $\vec{x} = (\mathscr{R}_x, \mathscr{Y}_x, \mathscr{C})$, the original image I is transformed to its $YCrCb$ representation, and $\vec{x}$ is applied to the Y channel, in order to obtain a Y_T intensity map, which is used to transform back to RGB, to obtain the resulting image T. The resulting images are evaluated according to the metrics $\mathscr{H}_Y$, $SSIM_R$, $SSIM_G$,

$SSIM_B$, which are the entropy of resulting images measured in the Y channel of the $YCrCb$ representation of these, and $SSIM_R, SSIM_G, SSIM_B$ are the $SSIM$ measures for original and resulting images using the R, G, B channels of the RGB representations of these. The non-dominated solutions are then stored in the Pareto set. $CMOPSO - CLAHE$ proccess is repeated until a criterion stop is reached.

5   Results and Discussion

Table 1: Initial parameters for CMOPSO-CLAHE.

Parameter	Value	Parameter	Value
$lower\_limit_{\mathscr{R}_x}$	2	$upper\_limit_{\mathscr{R}_x}$	$M/2$
$lower\_limit_{\mathscr{R}_y}$	2	$upper\_limit_{\mathscr{R}_y}$	$N/2$
$lower\_limit_{\mathscr{C}}$	0	$upper\_limit_{\mathscr{C}}$	0.5
Ω	100	t_{max}	100
$c_1\ min$	1.5	$c_1\ max$	2.5
$c_2\ min$	1.5	$c_2\ max$	2.5
$r_1\ min$	0.0	$r_1\ max$	1.0
$r_2\ min$	0.0	$r_2\ max$	1.0

Tests were performed using 8 color images from the dataset available at http://www.vision.caltech.edu/archive.html. Table 1 shows how $SMPSO$ was configured for the tests. $SMPSO$ implementation is available at [17], meanwhile the implementations for $CLAHE$, $\mathscr{H}$ and $SSIM$ are available at [18]. For every test image, 50 test were performed, and 10 non-dominated solutions were found in average. From Figures (1a,1b,1c) it is noticeable how CE is achieved; there is also a compromise relation between $\mathscr{H}$ and $SSIM_R, SSIM_G, SSIM_B$. It is noteworthy from Figure (1c) how higher values of $\mathscr{H}$ degrade images severely, so it is neccesary to find the correct balance between $\mathscr{H}$ and $SSIM_R, SSIM_G, SSIM_B$. In Figure (1d) it is shown the resultant image enhanced using the proposal described in [9]; it is noticeable that the resultant image does not achieve good CE; this is because the mono-objective approach does not use color information properly, and this result is the same for other test images. In Table 3, the non-dominated metric coefficients are shown, and in the last line it is shown the metric coefficients for image (1a), enhanced using the mono-objective proposal.

Although its metrics seem to fall in the Pareto Front, the visual information obtained is not enough to state that the mono-objective proposal is feasible for color images. These results are similar for every test image used.

(a) Original Image. $\mathcal{H}_{2y} = 0.207231$, $SSIM_R = 1$, $SSIM_G = 1$, $SSIM_B = 1$

(b) Enhanced Image. $\mathcal{H}_{2y} = 0.611275$, $SSIM_R = 0.00897331$, $SSIM_G = 0.00823064$, $SSIM_B = 0.00851013$

(c) Enhanced Image. $\mathcal{H}_{2y} = 0.0350595$, $SSIM_R = 0.416776$, $SSIM_G = 0.403636$, $SSIM_B = 0.417654$

(d) Enhanced Image using [9]. $\mathcal{H}_{2y} = 0.788927$, $SSIM_R = 0.000204143$, $SSIM_G = 0.0000526475$, $SSIM_B = 0.0000518143$

Figure 1: Original and resultant images of House 1

Table 2: Correlation table between metrics. Data was taken from Table 3.

Metrics	$\mathcal{H}_{2y}$	$SSIM_R$	$SSIM_G$	$SSIM_B$
$\mathcal{H}_{2y}$	1			
$SSIM_R$	-0.9826	1		
$SSIM_G$	-0.9823	0.9999	1	
$SSIM_B$	-0.9826	0.9999	0.9999	1

Table 3: Metric coefficients obtained using our approach for some non-dominated results from image in Figure (1), and the coefficients obtained using the approach of [9], shown in the last line.

|	$\mathscr{H}_{\mathscr{y}}$	$SSIM_R$	$SSIM_G$	$SSIM_B$
Result 1	0,455146	0,9844962	0,9859005	0,9850636
Result 2	0,341423	0,99448887	0,99505806	0,99470544
Result 3	0,9574285	0,605344	0,619333	0,60158
Result 4	0,9634576	0,598325	0,611372	0,597308
Result 5	0,9649405	0,583224	0,596364	0,582346
Result 6	0,388725	0,99102669	0,99176936	0,99148987
Result 7	0,9657106	0,579052	0,591965	0,578109
Result Mono	0,211073	0,999795857	0,9999473525	0,9999481857
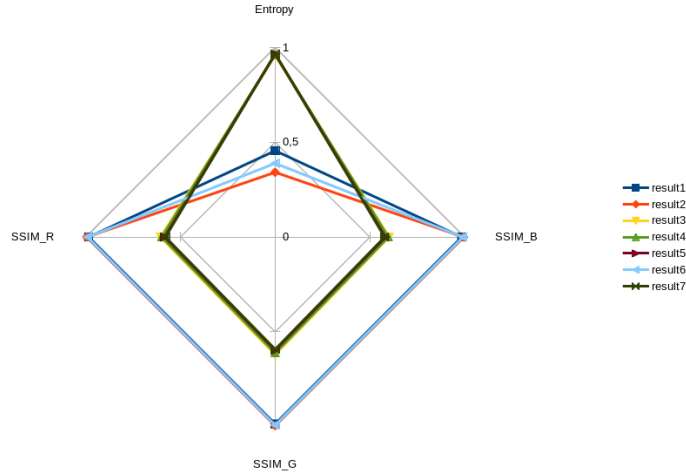
Figure 2: Pareto front drawn using data from Table 3

Figure (2) shows the Pareto Front created from the data in Table 3, and also Table 2 shows the correlation between metrics, analized from the results in Table 3. It is remarkable that there is a strong positive correlation between $SSIM_R$, $SSIM_G$ and $SSIM_B$; and there is a negative correlation between the previously mentioned metrics and $\mathscr{H}_{\mathscr{y}}$. These correlations indicate that the channels R, G, B of images are directly affected by the proccess that modifies Y channel (see Algorithm (1)). This also indicates that CE of color images can be posed as a bi-objective optimization problem, using only $\mathscr{H}_{\mathscr{y}}$ and $SSIM$ applied over Y channel.

6 Conclusion

A Multi-Objective approach for Contrast Enhancement of color images is presented, which takes into account intensity and color information as Multi-Objective metrics. This approach achieves several resultant images, with different compromise rates between contrast and structural-similarity, in order to maximize information available for further analysis.

The authors are still performing test with similar images found in the database. As future work, it would be useful to analyse the parameters used for the meta-heuristics, the use of non-marginal metrics to assess the resultant images obtained with the approach, and perform tests posing CE of color images as a bi-objective optimization problem.

References

[1] Kunio Doi. Computer-aided diagnosis in medical imaging: historical review, current status and future potential. *Computerized medical imaging and graphics*, 31(4):198–211, 2007.

[2] Avinash C Kak and Malcolm Slaney. *Principles of computerized tomographic imaging*. SIAM, 2001.

[3] Robert R Edelman and Steven Warach. Magnetic resonance imaging. *New England Journal of Medicine*, 328(10):708–716, 1993. PMID: 8433731.

[4] Thomas Lillesand, Ralph W Kiefer, and Jonathan Chipman. *Remote sensing and image interpretation*. John Wiley & Sons, 2014.

[5] Rafael C. Gonzalez and Richard E. Woods. *Digital Image Processing (2nd Ed)*. Prentice Hall, 2002.

[6] Stephen M Pizer, E Philip Amburn, John D Austin, Robert Cromartie, Ari Geselowitz, Trey Greer, Bart ter Haar Romeny, John B Zimmerman, and Karel Zuiderveld. Adaptive histogram equalization and its variations. *Computer vision, graphics, and image processing*, 39(3):355–368, 1987.

[7] Karel Zuiderveld. Contrast limited adaptive histogram equalization. In *Graphics gems IV*, pages 474–485. Academic Press Professional, Inc., 1994.

[8] Yeong-Taeg Kim. Contrast enhancement using brightness preserving bi-histogram equalization. *IEEE Transactions on Consumer Electronics*, 43(1):1–8, Feb 1997.

[9] LG Moré and MA Brizuela. Pso applied to parameter tuning of clahe based on entropy and structural similarity index.

[10] Luis G More, Marcos A Brizuela, Horacio Legal Ayala, Diego P Pinto-Roa, and Jose Luis Vazquez Noguera. Parameter tuning of clahe based on multi-objective optimization to achieve different contrast levels in medical images. In *Image Processing (ICIP), 2015 IEEE International Conference on*, pages 4644–4648. IEEE, 2015.

[11] F. Saitoh. Image contrast enhancement using genetic algorithm. In *Systems, Man, and Cybernetics, 1999. IEEE SMC '99 Conference Proceedings. 1999 IEEE International Conference on*, volume 4, pages 899–904 vol.4, 1999.

[12] Pourya Hoseini and Mahrokh G. Shayesteh. Efficient contrast enhancement of images using hybrid ant colony optimisation, genetic algorithm, and simulated annealing. *Digital Signal Processing*, 23(3):879 – 893, 2013.

[13] Rafael C Gonzalez and Richard E Woods. Processing, 2002.

[14] Antonio J Nebro, Juan José Durillo, Jose Garcia-Nieto, CA Coello Coello, Francisco Luna, and Enrique Alba. Smpso: A new pso-based metaheuristic for multi-objective optimization. In *Computational intelligence in miulti-criteria decision-making, 2009. mcdm'09. ieee symposium on*, pages 66–73. IEEE, 2009.

[15] A. Khellaf, A. Beghdadi, and H. Dupoisot. Entropic contrast enhancement. *IEEE Transactions on Medical Imaging*, 10(4):589–592, Dec 1991.

[16] Zhou Wang, Alan C Bovik, Hamid R Sheikh, and Eero P Simoncelli. Image quality assessment: from error visibility to structural similarity. *IEEE transactions on image processing*, 13(4):600–612, 2004.

[17] Juan J Durillo, Antonio J Nebro, and Enrique Alba. The jmetal framework for multi-objective optimization: Design and architecture. In *Evolutionary Computation (CEC), 2010 IEEE Congress on*, pages 1–8. IEEE, 2010.

[18] Gary Bradski. The opencv library. *Dr. Dobb's Journal: Software Tools for the Professional Programmer*, 25(11):120–123, 2000.